Control of Three-Phase Inverter for AC Motor Drive With Small DC-Link Capacitor Fed by Single-Phase AC Source

Hyun-Sam Jung, Seung-Jun Chee, *Student Member, IEEE*, Seung-Ki Sul, *Fellow, IEEE*, Young-Jae Park, Hyun-Soo Park, and Woo-Kyu Kim

***Abstract*—If a small dc-link capacitor is used in the dc link fed by a single-phase ac source, then the dc-link voltage severely fluctuates at twice of the source frequency. To handle this fluctuation, the concept of "average voltage constraint" is proposed in this study. On the basis of this concept, a flux-weakening scheme, generating the d-axis current reference $(i_{ds}^{r}{}^{*})$ for the interior permanent-magnet synchronous machine, is devised. The q-axis current reference $(i_{qs}^{r}{}^{*})$ is modified for the unity power factor operation in the viewpoint of an ac source without an additional sensor. The proposed scheme has been applied to the inverter-driven 1-kW compressor of an air conditioner. From the experimental results, it has been verified that the compressor operates well at the required operating condition, regardless of the severe fluctuation of dc-link voltage, because of the reduced dc-link capacitance. The frequency spectrum of the ac source current reveals that the harmonics of the source current meet the regulation of IEC 61000-3-2 Class A and that the overall power factor is above 96% without any additional circuit, such as an input filter and a power factor correction circuit.**

***Index Terms*—Capacitors, electrolytic capacitorless inverter, flux-weakening operation, harmonics regulation, home appliance, interior permanent-magnet synchronous motor (IPMSM), inverter, power factor, variable-speed drives, voltage constraint.**

I. Introduction

THE DC-LINK capacitor with large capacitance of several hundred or thousand microfarads is generally used to keep the dc-link voltage almost constant in a few kilowatt ac–dc–ac power conversion system fed by a single-phase ac source. The electrolytic capacitors generally have been used as dc-link capacitors in this system because of the large capacitance per unit volume. Due to the large capacitance in the dc link, the ac source current $I_{\rm in}$ is severely distorted and the input power factor is deteriorated. In addition, a huge inrush current flows through a rectifier to the capacitor at turning on the drive system. In order to deal with these issues, the additional circuits, such as a power factor correction circuit, an input filter, and a precharging circuit, are normally employed.

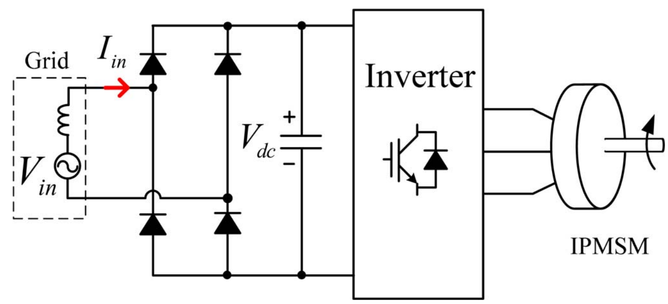

Fig. 1. Conceptual structure of the inverter system for home appliance.

Furthermore, the use of an electrolytic capacitor has a fatal weakness in reliability [1]. The electrolytic capacitor is the most fragile component in the power conversion system. In other words, the lifetime of the system is mainly dependent on that of the electrolytic capacitor. To improve the reliability of system, the methods of monitoring the capacitor status have been researched, which detect the end-of-life status of the capacitor for preventive maintenance [1]–[3].

To overcome the problems aforementioned, the matrix topology, which basically does not need the dc-link capacitor, has been researched. This topology is to perform the power conversion directly from the ac source to the ac load without any intermediate dc link. However, it needs a large amount of unidirectional switches to implement its bidirectional switches, which makes the control very complex [4]. Furthermore, it cannot be applicable to the power conversion system fed by a single-phase ac source.

In addition, there have been some efforts to use the film capacitor with small capacitance as the dc-link capacitor in an ac–dc–ac power conversion system [5]–[20]. This kind of system is thus called "electrolytic capacitorless system," which will be briefly called "capacitorless system" in this paper. This topology uses the film capacitor with several microfarads, instead of the electrolytic capacitor with several hundred or

Manuscript received June 15, 2013; accepted August 9, 2013. Date of publication November 1, 2013; date of current version March 17, 2014. Paper 2013-IDC-522, presented at the 2012 IEEE Energy Conversion Congress and Exposition, Raleigh, NC, USA, September 15–20, and approved for publication in the IEEE TRANSACTIONS ON INDUSTRY APPLICATIONS by the Industrial Drives Committee of the IEEE Industry Applications Society.
H.-S. Jung is with Samsung Heavy Industries Company, Ltd., Hwasung 445-330, Korea (e-mail: hyunsam.jung@samsung.com).
S.-J. Chee and S.-K. Sul are with the School of Electrical Engineering and Computer Science, Seoul National University, Seoul 151-742, Korea (e-mail: cheesj80@eepel.snu.ac.kr; sulsk@plaza.snu.ac.kr).
Y.-J. Park and W.-K. Kim are with Samsung Electronics Company, Ltd., Suwon 443-743, Korea (e-mail: dtl74.park@samsung.com; wookyu.kim@samsung.com).
H.-S. Park is with Samsung Electronics Company, Ltd., Suwon 443-743, Korea, and also with Sungkyunwan University, Suwon 440-746, Korea (e-mail: greenbee@samsung.com).
Color versions of one or more of the figures in this paper are available online at http://ieeexplore.ieee.org.
Digital Object Identifier 10.1109/TIA.2013.2288238

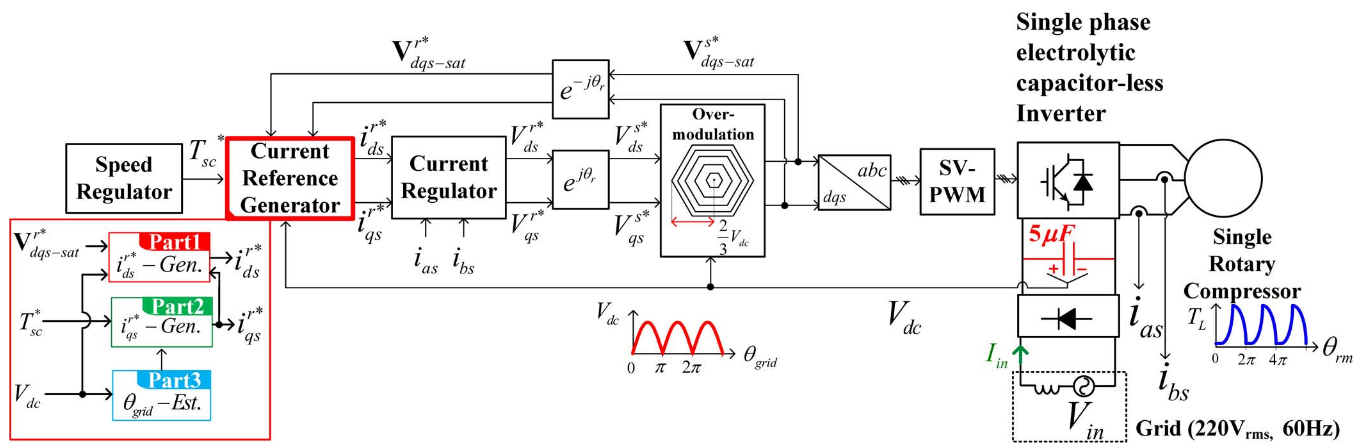

Fig. 2. Overview of the system with the proposed current reference generation.

several thousand microfarads, as the dc-link capacitor. The volume of the capacitorless system is dramatically reduced, and the reliability of system is enhanced, as compared to the power conversion system with the electrolytic capacitor. Additionally, the precharging circuit might be eliminated. It also leads to the cost and size reduction.

Researches about the capacitorless system can be divided into two kinds, according to the input ac source type, i.e., three-phase ac source and single-phase ac source. There are many researches about the capacitorless system with a three-phase ac source [5]–[16], whereas only a few papers deal with the capacitorless system fed by a single-phase ac source [17]–[20]. In this paper, the new control scheme is proposed for a single-phase ac source.

Fig. 1 shows the generic structure that is commonly used in home appliances such as an air conditioner. Generally, as the dc-link capacitor, the electrolytic capacitor with a range of $500-5000$ μF is employed, according to its rated power, to keep the dc-link voltage as constant V_{dc}. If a capacitor with several microfarads is employed as the dc-link capacitor in the case of the capacitorless system fed by a single-phase ac source, then the dc-link voltage fluctuates at twice of the ac source voltage frequency and the dc-link voltage is almost the rectified version of the ac source voltage. There were some researches to overcome this problem by modifying current references of the inverter. These conventional methods can be mainly divided into two types. One approach, which has been reported in [17], is that the shape of the q-axis current reference is modified as the square of sinusoidal wave synchronized with ac source voltage angle, and the other approach is in [19], where the q-axis current reference is shaped as a trapezoidal waveform. The former method improves the overall power factor. However, measuring the input voltage was required for the synchronization. In addition, the latter method reduced the low-order harmonic of speed ripples, but this method is worse than the former method, in terms of the harmonics spectrum of ac source current and the overall power factor. The d-axis current reference generated by both methods is determined by motor parameters, measured dc-link voltage, and tuning constants. These conventional methods are not only vulnerable to the parameter errors but also difficult to tune variables or gains. Furthermore, the experimental results of the previous researches cannot satisfy the regulation, i.e., IEC 61000-3-2 Class A, which is mandatory to an air conditioner.

To solve the aforementioned problems and to enhance the performance of conventional methods, a new control method is proposed in this paper. The d-axis current in the rotor reference frame $i_{ds}^{r\,*}$ is generated through the state feedback control based on the concept of "average voltage constraint." In addition, the q-axis current in the rotor reference frame $i_{qs}^{r\,*}$ is modified to maximize the ac source power factor without an additional sensor. Thus, it achieves not only the robustness to the parameter error but also the cost effectiveness. This scheme is applied to the inverter-driven 1-kW compressor of an air conditioner fed by a single-phase ac source. The validity and feasibility of the proposed control scheme have been proved by series of the experimental tests with a commercial air conditioner.

II. Proposed Control Method

The overall control block diagram is shown in Fig. 2. Three controllers, i.e., speed regulator, current reference generator, and current regulator, are connected in cascade. The current reference generator consists of three parts, which are interlinked with other parts. Each part of the reference current generator block is described here.

A. d-Axis Current Reference Generator: Part 1

As mentioned in the introduction, the dc-link voltage of a target system severely fluctuates at twice the frequency of the source voltage. To handle this problem, a new concept of "average voltage constraint" is introduced. The "average voltage" is the mean value of the fluctuating dc-link voltage during a half period of the source voltage represented on the d, q-axis current plane. The voltage is used as the constraint applied to the flux-weakening controller, which generates the d-axis current reference.

Assuming that the d-axis current varies slowly enough to be approximated as a constant, the available average q-axis current for a half period of ac source voltage, i.e., $i_{qs\text{-av}}^{r}$, can be derived from the voltage equation of the interior permanent-magnet

TABLE I
MACHINE PARAMETER

Quantity	Abbreviation	Value[unit]
Pole Number	P	4
Stator resistance	Rs	0.4775 [Ω]
Synchronous inductance at the d-axis	Ld	6.11 [mH]
Synchronous inductance at the q-axis	Lq	8.17 [mH]
Flux linkage	λ_{pm}	0.1 [V/(rad/s)]
Rated power	Prated	1 [kW]
Rated speed	ω_{rated}	5400 [r/min]
Inertial	J	0.5 [mkgm2]

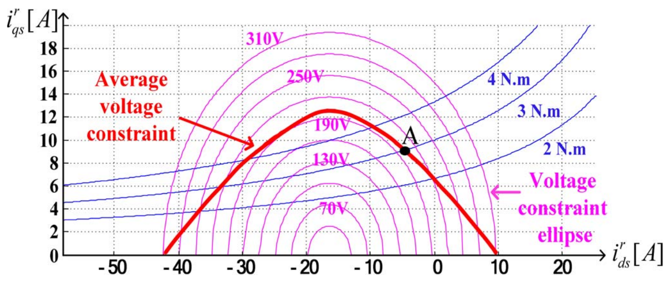

Fig. 3. Concept of the average voltage constraint curve.

synchronous motor (IPMSM) and the voltage constraint of the three-phase inverter [21], as follows:

$$V^r_{ds} = Ri^r_{ds} + L_d \frac{di^r_{ds}}{dt} - \omega_r L_q i^r_{qs}$$
$$V^r_{qs} = Ri^r_{qs} + L_q \frac{di^r_{qs}}{dt} + \omega_r \left(\lambda_{\rm pm} + L_d i^r_{ds}\right) \tag{1}$$
$$\frac{V_{\rm dc}}{\sqrt{3}} \geq \sqrt{{V^r_{ds}}^2 + {V^r_{qs}}^2} \tag{2}$$
$$i^r_{qs\text{-av}} = \frac{1}{\pi}\int_0^{\pi} \frac{1}{\omega_r L_q}\sqrt{\frac{V_{\rm dc}(\theta)^2}{3} - {V^r_{qs}}^2 d\,\theta}. \tag{3}$$

The average voltage constraint curve at 5400 r/min in the case of the IPMSM with parameters listed in the Table I is represented on the d, q-axis current plane, as shown in Fig. 3. The conventional flux-weakening control makes the d-axis current reference fluctuate, in accordance with the dc-link voltage as voltage constraint ellipse. Previous researches also have generated the d-axis current reference based on this principle. However, this principle is not appropriate to the capacitorless IPMSM drive system. Periodical dc-link voltage fluctuation makes the d-axis current reference fluctuate, and the fluctuation of the d-axis current reference aggravates the lack of voltage margin for synthesizing reference current. Therefore, with this chain reaction, the current regulation performance rapidly deteriorates. To deal with this problem, a new flux-weakening control scheme for the capacitorless system is proposed in this paper. In the proposed scheme, the d-axis current reference is determined at the crossing point of the average voltage constraint loci and the constant torque loci. The d-axis current reference at the crossing point guarantees the average of torque required to control the speed of the compressor, although the q-axis current varies according to the dc-link voltage during the half period of ac source. As an example, if the average torque, which is required to control the speed of the compressor, is 3 N · m, the d-axis current would be determined at point "A" in this concept, as shown in Fig. 3. The d-axis current is limited between null (no flux weakening) and the equivalent permanent magnet current (null flux), such as $(-\lambda_{\rm pm}/L_d < i^{r*}_{ds} < 0)$, which is implemented as a limiter in Fig. 4.

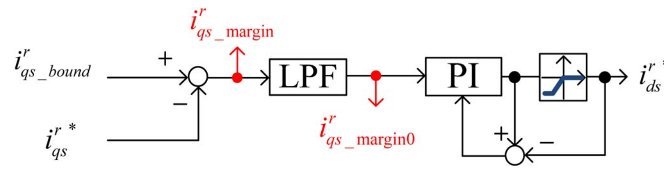

Fig. 4. d-axis current reference generator.

The input of this reference generator, i.e., $i^r_{qs\_\rm bound}$, is defined by (4)–(6). In these equations, $\mathbf{V}^{r*}_{dqs\text{-sat}} = V^{r*}_{ds\text{-sat}} + jV^{r*}_{qs\text{-sat}}$ is the voltage applied to the IPMSM after the overmodulation of the pulsewidth modulation inverter, as shown in Fig. 2. The voltages are bounded from the hexagon in the voltage plane, and the size of the hexagon varies according to the dc-link voltage. The meaning of $i^r_{qs\_\rm bound}$ is the synthesizable current in this bounded voltage. The other input of this reference generator, i.e., i^{r*}_{qs}, is the current reference for the torque generation of the IPMSM, which is set by the speed controller. To generate i^{r*}_{ds} based on the constraint with these inputs, a proportional–integral (PI) controller and a first-order low-pass filter (LPF) are used, as shown in Fig. 4. This LPF is used to obtain the average value of $i^r_{qs\_\rm margin}$, which is fluctuating at twice of the ac source frequency. Therefore, the cutoff frequency of the LPF should be low enough to block this 120-Hz component and to extract the quasi-dc component, i.e., $i^r_{qs\_\rm margin0}$. The PI controller makes the $i^r_{qs\_\rm margin0}$ follow its reference $i^{r*}_{qs\_\rm margin0}$, by determining the d-axis current. This $i^{r*}_{qs\_\rm margin0}$ is normally set as zero. As a result, the voltage margin is guaranteed for synthesizing the q-axis current reference, averagely. That is,

$$V^r_{ds\_\rm bound} = \sqrt{\frac{V^2_{\rm dc}}{3} - {V^{r*}_{qs\text{-sat}}}^2} \tag{4}$$
$$K_z = \text{LPF}\left(\left(-V^{r*}_{ds\text{-sat}} + R_s i^r_{ds}\right)/i^r_{qs}\right) \tag{5}$$
$$i^r_{qs\_\rm bound} = V^r_{ds\_\rm bound}/K_z. \tag{6}$$
$$T_e = \frac{3}{2}\frac{P}{2}\left[\lambda_{\rm pm} + (L_d - L_q)i^r_{ds}\right] i^r_{qs}. \tag{7}$$

The gains of this PI controller can be set physically by deriving the transfer function of $i^r_{qs\_\rm margin0}/i^{r*}_{qs\_\rm margin0}$, under the assumption that $i^r_{qs\_\rm bound}$, which comes from the average voltage constraint in Fig. 3, is linear, as follows:

$$i^r_{qs\_\rm bound} = A_{e0} i^r_{ds} + B_{e0}. \tag{8}$$

This assumption is reasonable because the average voltage constraint, which is represented in the current plane, is almost linear in most of the operating region, i.e., $-\lambda_{\mathrm{pm}}/L_d < i_{ds}^{r*} < 0$, as shown in Fig. 3. If the bandwidth of the current regulator, i.e., ω_{cc}, is fast enough and the current vector i_{dqs}^r well matches to its reference $i_{dqs}^r{}^*$, then the inverter can be considered by unity gain. In steady state, $i_{qs\_\mathrm{margin0}}^r$ is approximated by the multiplication of i_{ds}^r and the gain A_{e0}. Thus, an open-loop transfer function of the d-axis current reference generator can be derived as

$$G_{\mathrm{fw}} = A_{e0} \times \frac{\omega_{\mathrm{lpf}}}{(s+\omega_{\mathrm{lpf}})} \times k_{\mathrm{pd\_ref}} \frac{(s + k_{\mathrm{id\_ref}}/k_{\mathrm{pd\_ref}})}{s}$$
$$= A_{e0}\omega_{\mathrm{lpf}} k_{\mathrm{pd\_ref}}/s \tag{9}$$

under the assumption

$$k_{\mathrm{id\_ref}}/k_{\mathrm{pd\_ref}} = \omega_{\mathrm{lpf}}.$$

In (9), ω_{lpf} stands for the cutoff frequency of the LPF in Fig. 4; $k_{\mathrm{id\_ref}}$ and $k_{\mathrm{pd\_ref}}$ represent the proportional and integral gains of the PI regulator in Fig. 3, respectively. As a result, the bandwidth of the d-axis current generator (ω_{dg}) can be deduced as

$$\frac{i_{qs\_\mathrm{margin0}}^r}{i_{qs\_\mathrm{margin0}}^{r*}} = \frac{G_{\mathrm{fw}}}{1+G_{\mathrm{fw}}} = \frac{\omega_{\mathrm{dg}}}{s+\omega_{\mathrm{dg}}} \tag{10}$$

where

$$\omega_{\mathrm{dg}} = A_{e0} k_{\mathrm{pd\_ref}} \omega_{\mathrm{lpf}}.$$

Thus, it is suggested that ω_{dg} should be slightly higher than the bandwidth of the speed regulator, i.e., ω_{sc}, and much lower than the bandwidth of the current regulator, i.e., ω_{cc}. With this guideline, the gains of the PI regulator in the $i_{ds}^r{}^*$ generator block in Fig. 4 can be set.

B. q-Axis Current Reference Generator: Part 2

The purpose of the part 2 is generating $i_{qs}^r{}^*$ to maximize the ac source power factor. If the unity power factor is assumed, the input power P_{in} should be the square of the sinusoidal function synchronized with the ac grid angle $\sin^2\theta_{\mathrm{grid}}$, under the assumption of sinusoidal ac source voltage. Because of negligible dc-link capacitance, the input power is the same as the output power instantaneously. Therefore, $i_{qs}^r{}^*$ can be derived as

$$P_{\mathrm{in}} = \|P_{\mathrm{in}}\| \sin^2\theta_{\mathrm{grid}}$$
$$P_{\mathrm{out}} = 1.5 \times \left(V_{ds}^r i_{ds}^r + V_{qs}^r i_{qs}^r\right)$$
$$= 1.5 \times \left(-\omega_r L_q i_{ds}^r + \omega_r \lambda_{pm} + \omega_r L_d i_{ds}^r\right) i_{qs}^r$$
$$P_{\mathrm{out}} = P_{\mathrm{in}}$$
$$i_{qs}^r = K_{\mathrm{temp}} \sin^2\theta_{\mathrm{grid}} \tag{11}$$

which has been derived under the assumption that a transient q-axis voltage, i.e., $L_q((di_{qs}^r)/(dt))$, is negligible and the current is regulated well enough according to its reference in average sense.

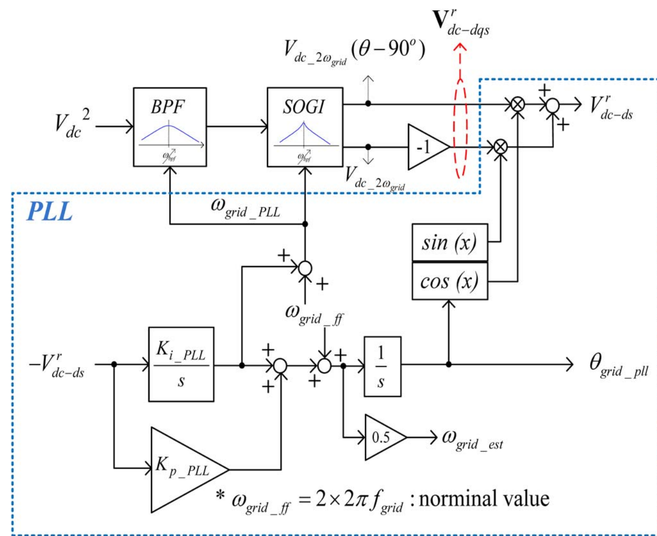

Fig. 5. Grid angle estimator.

For the speed control, the average torque for a half period of ac source voltage should be regulated, although the current reference is modified. In addition, the following equation should be satisfied:

$$\int_{\frac{T_{\mathrm{grid}}}{2}} i_{qs}^r{}^* = \int_{\frac{T_{\mathrm{grid}}}{2}} i_{qs\_\mathrm{SC}}^r{}^* \tag{12}$$

where $i_{qs\_\mathrm{SC}}^r{}^*$ is the output of the speed regulator, and T_{grid} is the period of the grid voltage.

The bandwidth of the speed regulator should be low enough to represent $i_{qs\_\mathrm{SC}}^r{}^*$ as the average value. From (12), K_{temp} can be set as

$$K_{\mathrm{temp}} = 2 \times i_{qs\_\mathrm{SC}}^r{}^*. \tag{13}$$

Finally, the q-axis current reference can be modified as

$$i_{qs}^r{}^* = 2 \times i_{qs\_\mathrm{SC}}^r{}^* \sin^2\theta_{\mathrm{grid}}. \tag{14}$$

C. Estimation of Grid Angle: Part 3

In order to generate $i_{qs}^r{}^*$, it is required to find out the grid angle θ_{grid}. To identify the grid angle, an additional voltage sensor, measuring input source voltage, had been used in earlier researches [17]–[20]. However, in this study, the grid angle is estimated without any additional hardware. The principle is based on the fact that the fluctuation of the dc-link voltage directly reflects the variation of the source voltage due to negligible dc-link capacitance. By exploiting this observation, the grid angle is extracted from the measured dc-link voltage based on a simple phase-locked loop (PLL).

The virtual stationary reference frame d, q-axis voltage $(\mathbf{V}_{\mathrm{dc\_}dqs}^s = V_{\mathrm{dc\_}ds}^s + jV_{\mathrm{dc\_}qs}^s)$ in (15), i.e., the input of the PLL, is defined by simple signal processing, such as bandpass

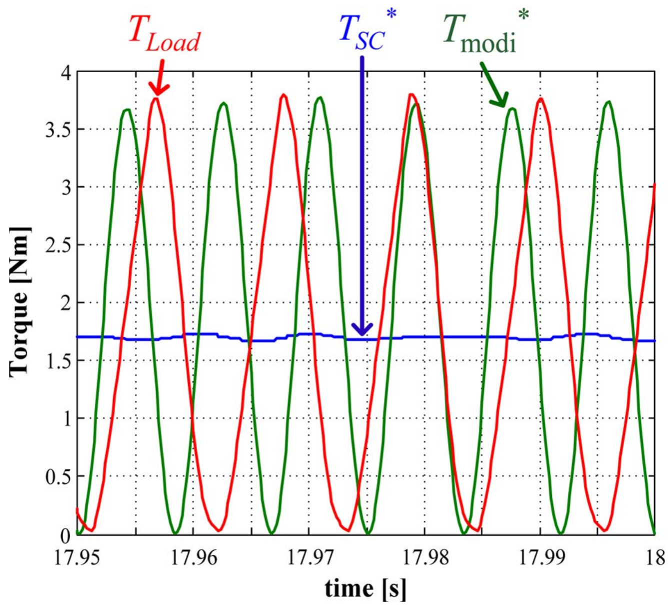

Fig. 6. Torque plot: torque reference from speed regulator $T_{\mathrm{sc}}{}^*$, torque reference modified by the proposed method $T_{\mathrm{modi}}{}^*$, and load torque of the compressor T_{Load}.

filter (BPF) and second-order general integrator (SOGI, i.e., [22]), which is shown in Fig. 5. That is,

$$V^s_{\mathrm{dc\_}ds} = V_{\mathrm{dc\_}2\omega_{\mathrm{grid}}}(\theta - 90^\circ)$$
$$V^s_{\mathrm{dc\_}qs} = -V_{\mathrm{dc\_}2\omega_{\mathrm{grid}}}. \tag{15}$$

III. Simulation Results

To verify the validity and feasibility of the proposed method, a computer simulation has been performed by MATLAB. The simulation parameters are listed in Table I. It is assumed that the load torque of a single rotary compressor at 5400 r/min, i.e., T_{Load}, looks similar to the load torque shown in Fig. 6. This value of T_{Load} is calculated to get about 1 kW of average of output power. The torque reference proportional to the current reference in (11), $T_{\mathrm{modi}}{}^*$, is also shown in Fig. 6. Because of the fluctuation of load torque and the fluctuation of torque reference, i.e., the q-axis current reference by (11), there are inevitable torque ripples in the IPMSM. The main frequency components of the ripple are $2\omega_{\mathrm{grid}} - \omega_{\mathrm{rm}}$ and $2\omega_{\mathrm{grid}} + \omega_{\mathrm{rm}}$. These ripples of torque are reflected as the speed ripples of the compressor, after being filtered out by large inertia of the compressor. In Fig. 7, it is shown that the speed ripple is slightly increased, as much as about 50 r/min, in the capacitorless system compared to the conventional compressor with large dc-link capacitance in the dc link. In spite of the reduced dc-link capacitance from 1000 to 5 μF, the speed ripple increased from 1% to 2%.

Fig. 8 shows the characteristics of the input current of three kinds of method: method 1 is the capacitorless inverter controlled by the proposed scheme in this paper; method 2 is the capacitorless system with the conventional control scheme in [17]; method 3 is the general inverter with 1000 μF controlled by the general current control scheme. As shown in Fig. 8, the harmonics spectrum of input current controlled by method 1 is the best among those of the three methods.

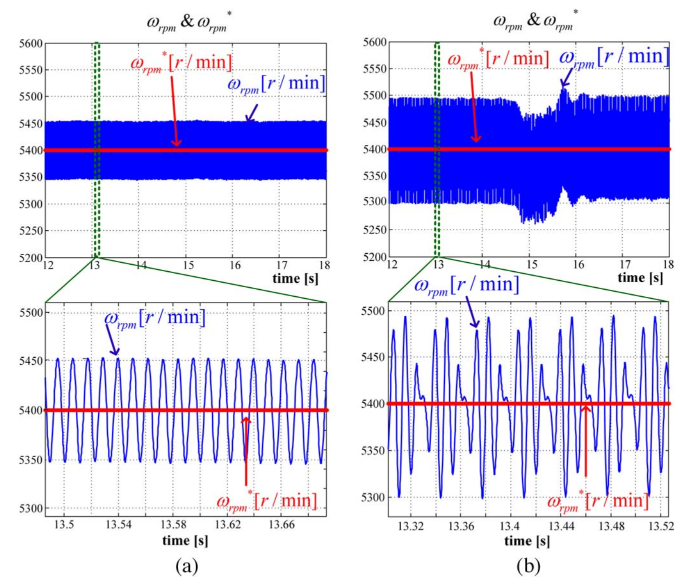

Fig. 7. Comparison of speed. (a) Speed ripple: general inverter with 1000-μF dc-link capacitor. (b) Speed ripple: capacitorless inverter with 5-μF dc-link capacitor controlled by the proposed control scheme.

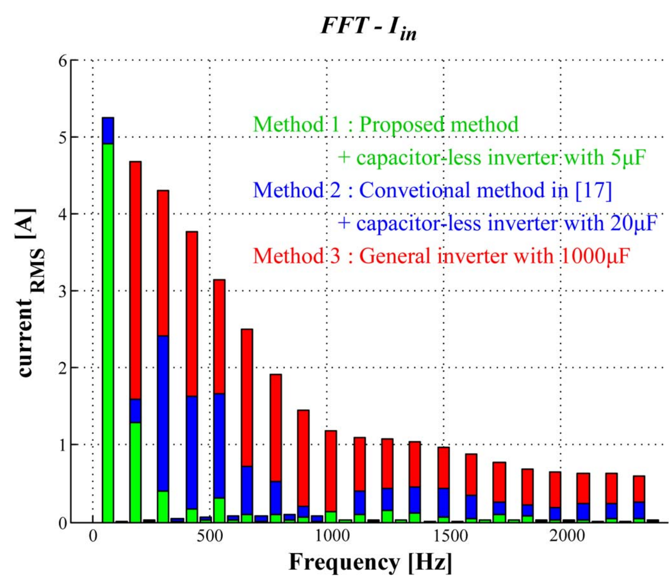

Fig. 8. Comparison of harmonics spectrum of input current ripple.

IV. Experimental Results

The configuration of the system, as aforementioned in Fig. 2, is implemented in Fig. 9. This system is the air conditioner with a single rotary compressor fed by a single-phase 220-V 60-Hz ac source. In addition, the rotor angle and speed of the IPMSM are estimated by using the sensorless control algorithm based on a back electromotive force observer [21]. The switching frequency of the inverter is set at 13 kHz. The 5-μF film capacitor is used as the dc-link capacitor of the inverter. The bandwidth of the current controller ω_{cc}, the bandwidth of the speed controller ω_{sc}, and the bandwidth of the

Fig. 9. Experimental setup (air conditioner).

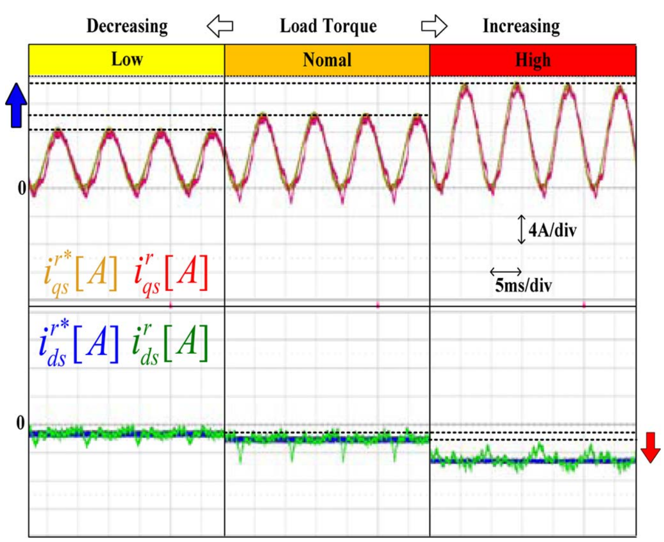

Fig. 10. Experimental result i_{dqs}^{r*} and i_{dqs}^{r}.

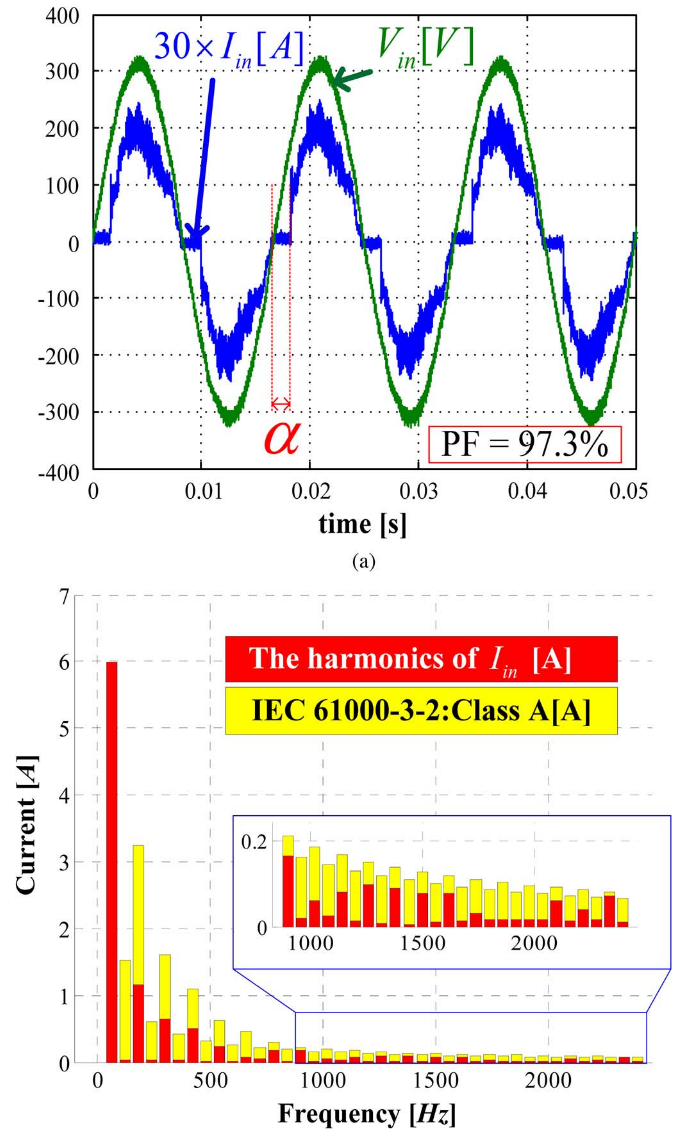

(a) (b)

Fig. 11. Experimental results. (a) Grid voltage ($V_{\rm in}$), input current ($I_{\rm in}$), and power factor (PF). (b) Harmonics of $I_{\rm in}$ and the regulation of IEC 61000-3-2: Class A.

d-axis current reference generator $\omega_{\rm dg}$ are 400 Hz, 1 Hz, and 20 Hz, respectively.

In order to verify the generation of $i_{ds}^{r}{}^{*}$ based on the average voltage constraint, the load torque is increased, maintaining operating speed, i.e., 5400 r/min. As shown in Fig. 10, as the load torque increases, $i_{ds}^{r}{}^{*}$ decreases. In addition, the validity of the proposed method can be proved by the characteristic of an input current waveform and its harmonics, as shown in Fig. 11, at a typical operating condition, a normal load torque, and 5400 r/min. The shape of the input current in Fig. 11(a) contains a section denoted by α, where the input current is not conducting. This section distorts the input current and makes the harmonics. However, these harmonics are still within the regulation limit, as shown in Fig. 11(b). The q-axis inductance voltage $L_q((di_{qs}^{r})/(dt))$, which is ignored when the shape of $i_{qs}^{r}{}^{*}$ is determined, results in the low-order harmonics. However, the increase of low-order harmonics from the q-axis inductance voltage has negligible impact on harmonics to the regulation limit because the regulation limit of low-order harmonics is large enough to allow that distortion. Therefore, the harmonics of the input current from the experimental result meets the regulation, i.e., IEC 61000-3-2 Class A [23]. In addition, the power factor in Fig. 12(a) reaches up to 97.3%.

The performance of the proposed method is tested at the overall speed range of the compressor. The results are shown in Fig. 12. When the proposed method is applied, the power factor has been kept above 96% at overall operating speed.

V. Conclusion

This paper has proposed a novel variable speed control strategy of the IPMSM, which is driven by an electrolytic capacitorless inverter fed by a single-phase ac source. First,

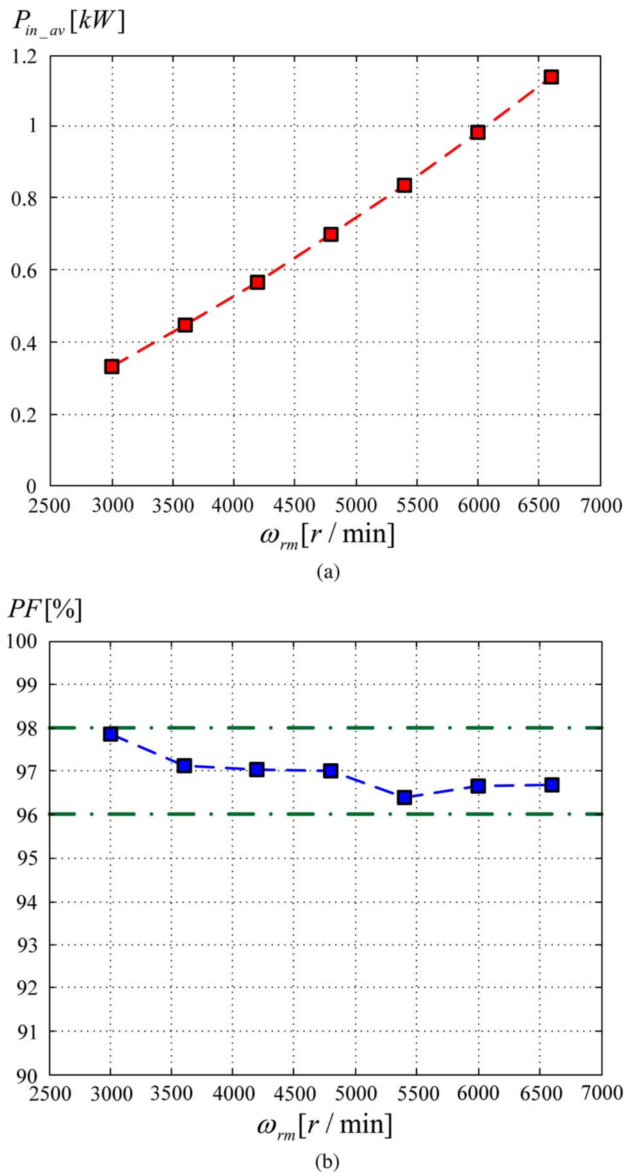

Fig. 12. Experimental results. (a) Average input power in the whole range of operating speed of the compressor. (b) Overall power factor in the whole range of operating speed of the compressor.

the concept of average voltage constraint is suggested as the virtual voltage constraint in the capacitorless inverter system. By generating $i_{ds}^{r}{}^*$ based on this constraint, the margin of the voltage for synthesizing $i_{qs}^{r}{}^*$ is always guaranteed. Second, the shape of $i_{qs}^{r}{}^*$ is modified for the unity power factor operation. To generate the modified $i_{qs}^{r}{}^*$, the grid angle and grid frequency are extracted from the dc-link ripple by using a PLL without an additional sensor. Therefore, to verify the validity of the proposed method, it is applied to an inverter-driven commercial air conditioner, whose compressor motor is an IPMSM. The electric source of the air conditioner is a single-phase 220-V_{rms} 60-Hz ac source. Although the dc-link capacitance is decreased down to 5 μF, the experimental results with 1-kW-level input power reveal the overall power factor above 96% and satisfaction of IEC 61000-3-2 Class A without any additional hardware. The proposed control scheme would extend the applicability of the capacitorless inverter to home appliance.

References

[1] A. M. Imam, T. G. Habetler, R. G. Harley, and D. M. Divan, "Condition monitoring of electrolytic capacitor in power electronic circuits using adaptive filter modeling," in *Proc. 36th IEEE PESC*, 2005, pp. 601–607.

[2] L. Kwang-Woon, K. Myungchul, Y. Jangho, L. Sang Bin, and Y. Ji-Yoon, "Condition monitoring of DC-link electrolytic capacitors in adjustable-speed drives," *IEEE Trans. Ind. Appl.*, vol. 44, no. 5, pp. 1606–1613, Sep./Oct. 2008.

[3] M. A. Vogelsberger, T. Wiesinger, and H. Ertl, "Life-cycle monitoring and voltage-managing unit for DC-link electrolytic capacitors in PWM converters," *IEEE Trans. Power Electron.*, vol. 26, no. 2, pp. 493–503, Feb. 2011.

[4] Y. Young-Doo and S. Seung-Ki, "Carrier-based modulation technique for matrix converter," *IEEE Trans. Power Electron.*, vol. 21, no. 6, pp. 1691–1703, Nov. 2006.

[5] C. Xiyou and M. Kazerani, "Space vector modulation control of an AC–DC–AC converter with a front-end diode rectifier and reduced DC-link capacitor," *IEEE Trans. Power Electron.*, vol. 21, no. 5, pp. 1470–1478, Sep. 2006.

[6] K. Lee, T. M. Jahns, G. Venkataramanan, and W. E. Berkopec, "DC-bus electrolytic capacitor stress in adjustable-speed drives under input voltage unbalance and sag conditions," *IEEE Trans. Ind. Appl.*, vol. 43, no. 2, pp. 495–504, Mar./Apr. 2007.

[7] Y. Hyunjae, S. Seung-Ki, J. Hoyong, and H. Youngho, "Design of a variable speed compressor drive system for air-conditioner without electrolytic capacitor," in *Conf. Rec. 42nd IEEE IAS Annu. Meeting*, 2007, pp. 305–310.

[8] M. E. de Oliveira Filho, J. R. Gazoli, A. J. S. Filho, and E. R. Filho, "A control method for voltage source inverter without dc link capacitor," in *Proc. IEEE PESC*, 2008, pp. 4432–4437.

[9] M. Hinkkanen and J. Luomi, "Induction motor drives equipped with diode rectifier and small DC-link capacitance," *IEEE Trans. Ind. Electron.*, vol. 55, no. 1, pp. 312–320, Jan. 2008.

[10] R. Maheshwari, S. Munk-Nielsen, and S. Busquets-Monge, "EMI performance comparison of two-level and three-level inverters in small dc-link capacitors based motor drives," in *Proc. IEEE ISIE*, 2012, pp. 652–657.

[11] J. S. Kim and S. K. Sul, "New control scheme for AC-DC-AC converter without DC link electrolytic capacitor," in *Proc. 24th IEEE PESC*, 1993, pp. 300–306.

[12] G. Bon-Gwan and N. Kwanghee, "A DC link capacitor minimization method through direct capacitor current control," in *Conf. Rec. 37th IEEE IAS Annu. Meeting*, 2002, vol. 2, pp. 811–817.

[13] R. M. Tallam, R. Naik, M. L. Gasperi, T. A. Nondahl, L. Hai Hui, and Y. Qiang, "Practical issues in the design of active rectifiers for AC drives with reduced DC-link capacitance," in *Conf. Rec. 38th IEEE IAS Annu. Meeting*, 2003, vol. 3, pp. 1538–1545.

[14] Y. Anno, S. Seung-Ki, K. Hyeseung, and K. Kyung-Seo, "Flux-weakening strategy of an induction machine driven by an electrolytic-capacitor-less inverter," *IEEE Trans. Ind. Appl.*, vol. 47, no. 3, pp. 1328–1336, May/Jun. 2011.

[15] C. R. Neuhaus and R. W. De Doncker, "DC-link voltage control for switched reluctance drives with reduced DC-link capacitance," in *Proc. IEEE ECCE*, 2010, pp. 4192–4198.

[16] L. Wook-Jin and S. Seung-Ki, "DC-link voltage stabilization for reduced dc-link capacitor inverter," in *Proc. IEEE ECCE*, 2009, pp. 1740–1744.

[17] I. Takahashi and H. Haga, "Power factor improvement of single-phase diode rectifier circuit by field-weakening of inverter-driven IPM motor," *Elect. Eng. Jpn.*, vol. 152, no. 2, pp. 66–73, Jul. 2005.

[18] H. Saren, K. Rauma, and O. Pyrhonen, "DTC driven single phase fed voltage source inverter with small dc-link capacitor," in *Proc. IEEE ISIE*, 2005, vol. 2, pp. 411–415.

[19] H. Lamsahel and P. Mutschler, "Permanent magnet drives with reduced dc-link capacitor for home appliances," in *Proc. 35th IEEE IECON*, 2009, pp. 725–730.

[20] K. Inazuma, K. Ohishi, and H. Haga, "High-power-factor control for inverter output power of IPM motor driven by inverter system without electrolytic capacitor," in *Proc. IEEE ISIE*, 2011, pp. 619–624.

[21] S. K. Sul, *Control of Electric Machine Drive Systems*. New York, NY, USA: Wiley, 2011, pp. 143, 250.

[22] M. Ciobotaru, R. Teodorescu, and F. Blaabjerg, "A new single-phase PLL structure based on second order generalized integrator," in *Proc. 37th IEEE PESC*, 2006, pp. 1–6.

[23] *Part 3-2: Limits—Limits for Harmonic Current Emissions (Equipment Input Current <= 16 A Per Phase)*, IEC Std. 61000-3-2, 2004.

Hyun-Sam Jung received the B.S. and M.S. degrees in electrical engineering and computer science from Seoul National University, Seoul, Korea, in 2010 and 2012, respectively.

Since 2012, he has been with Samsung Heavy Industries Company, Ltd., Hwasung, Korea. His current research interests include power electronics control of electrical machines and power-converter circuits.

Seung-Jun Chee (S'12) was born in Korea in 1980. He received the B.S. and M.S. degrees in electrical engineering in 2003 and 2005, respectively, from Seoul National University, Seoul, Korea, where he is currently working toward the Ph.D. degree in electrical engineering.

In 2005, he joined Samsung Electronics Company, Ltd., where he worked for six years. His current research interests include power electronic control of electrical machines and power-converter circuits.

Seung-Ki Sul (S'78–M'80–SM'98–F'00) received the B.S., M.S., and Ph.D. degrees from Seoul National University, Seoul, Korea, in 1980, 1983, and 1986, respectively, all in electrical engineering.

From 1986 to 1988, he was an Associate Researcher with the Department of Electrical and Computer Engineering, University of Wisconsin, Madison, USA. From 1988 to 1990, he was a Principal Research Engineer with Gold-Star Industrial Systems Company, Korea. Since 1991, he has been a member of the faculty in the School of Electrical Engineering, Seoul National University, where he is currently a Full Professor. From 2003 to 2004, he was a Research Director and an Acting Consultant with Yaskawa Electric Company, Japan. From 2005 to 2007, he was the Vice Dean of the Engineering College, Seoul National University. In addition, from 2008 to 2011, he was the President of the Electrical Engineering Science Research Institute funded by the Korean Government. He has published over 120 reviewed journal papers, which are mainly in IEEE TRANSACTIONS. His current research interests include power electronic control of electrical machines, electric/hybrid vehicle and ship drives, and power-converter circuits for renewal energy sources.

Prof. Sul was the Technical Chair of the IEEE Power Electronics Specialists Conference in 2006 and the General Chair of the IEEE ECCE Asia 2011. He is currently the Editor-in-Chief of the *Journal of Power Electronics*, which is an SCIE-registered journal, published by the Korean Power Electronics Institute, Seoul, Korea.

Young-Jae Park received the B.S. and M.S. degrees in electrical and electronics engineering from Yonsei University, Seoul, Korea, in 1998 and 2001, respectively.

He is currently with the Digital Media and Communication R&D Center, Samsung Electronics Company Ltd., Suwon, Korea. His current research interests include control theory and its applications to electric machines.

Hyun-Soo Park was born in Seoul, Korea, on August 22, 1970. He received the B.S. and M.S. degrees in electrical engineering from Yonsei University, Seoul, Korea, in 1993 and 1995, respectively. He is currently working toward the Ph.D. degree at Sungkyunwan University, Suwon-si, Korea.

In 1995, he joined the Digital Media and Communication R&D Center, Samsung Electronics Company Ltd., Suwon, Korea, where he has developed large-scale integrators and algorithms, including data processor, phase-locked loop, and partial response maximum likelihood types. His current research topics are related to power electronics for home appliances.

Woo-Kyu Kim received the M.S. and Ph.D. degrees in precision machinery engineering from The University of Tokyo, Tokyo, Japan, in 1995 and 1999, respectively.

In 2002, he joined the Digital Media and Communication R&D Center, Samsung Electronics Company, Ltd., Suwon, Korea. He has developed technology in the field of printers and home appliances. His current research topics are related to home robot cleaners and power efficiency of system air-conditioners.